Technical Sciences
Academy of Romania
www.jesi.astr.ro

Journal of Engineering Sciences and Innovation
Volume 5, Issue 4 / 2020, pp. 339-352

C. Environmental Engineering and Energy

Received **10 September 2020** Accepted **12 November 2020**
Received in revised from **21 October 2020**

Wind resource assessment system based on time-scale-dependent roughness

CRISTIAN SUTEANU*

Department of Geography & Environmental Studies and
Department of Environmental Science,
Saint Mary's University, 923 Robie St., Halifax, NS, Canada

Abstract. Wind speed intermittence and its forms of pattern change represent sources of significant uncertainties related to wind power. This article introduces a methodological system designed to contribute to an effective assessment of wind resources, by complementing the current wind speed evaluation procedures with the capability of capturing time-scale-dependent pattern properties. The proposed approach to nonstationary wind speed time series produces a comprehensive picture of the wind patterns, in which wind speed variability is quantitatively explored in terms of both time and temporal scale. This approach can thus support responses to the challenges posed by the task of assessing and comparing locations for wind turbines and wind farms, especially in the context of pattern changes in wind resources expected to occur due to climate change.

Keywords: wind energy, wind variability, time scale, time series roughness.

1. Introduction

The challenges involved by climate change and the worldwide increasing energy demand contribute to a growing importance of renewable energy sources. In this context, wind energy is particularly attractive [1], especially if applied in combination with other renewable sources, such as solar and wave energy [2]. Wind energy has a low contribution to air pollution compared to other energy sources, and its carbon footprint is remarkably small; moreover, it does not contribute to a deepening of the water crisis, which was identified as one of the major global risks of the future [3]. Overall, the robust development of wind power has major positive effects on sustainability [4].

*Correspondence address: Cristian.Suteanu@smu.ca

Like all energy sources, wind energy also has its limitations. One of the most important ones is caused by the intermittent nature of wind [5-7]. In fact, wind speed variability represents the main natural component of the uncertainty affecting this energy source. Addressing intermittency already involves a range of solutions [8], but they contribute to the cost of energy: therefore, it is important to accurately assess intermittency and minimize its effects. Numerous statistical methods have been applied for the evaluation of wind speed variability, starting with the coefficient of variation, statistical moments of second, third, and fourth order, the range divided by the weighted average of the quartiles, etc., to more robust statistics, such as the median absolute deviation divided by the weighted average of quartiles, the median absolute deviation normalized by the median, etc. [9]. While these methods differ from each other in many ways, they all focus on sets of wind speed values, without taking in consideration the succession of these values in the time series. More detailed approaches to wind speed patterns, such as wind speed distributions, offer a more comprehensive picture of wind patterns [10], but they do not convey any information on the way the wind speed values are actually distributed in time.

However, as this paper will show, depending on the goal of wind speed pattern analysis, the temporal succession of the time series values can be crucially important for the way in which wind turbines operate, and their overall effectiveness. A realistic and comprehensive evaluation of wind patterns, performed, for instance, in order to assess potential locations for a wind farm, or to compare locations for individual wind turbines, cannot ignore the effects created by the temporal succession of wind speed values.

Wind variability is expressed on a wide range of time scales, from under one second to months, years, etc. [6, 11] On a sub-second to second range, wind variability is important for the wind turbine loading, which varies as a function of both time and height: turbine design must take these dynamic aspects of wind flow in consideration. On a scale of hours to days to months and more, implications of wind variability affect energy availability. Acquiring information on scale-dependent characteristics of wind patterns becomes particularly relevant when the wind turbine is considered from the point of view of its energy conversion effectiveness.

On the other hand, climate change is involving significant change to wind patterns [12-14]. Not only is the overall wind potential affected: its variability is also changing; moreover, the ranges of time scales on which such changes occur suffer transformations in their turn [15, 16].

For these reasons, beyond the mentioned commonly assessed statistical aspects of wind speed patterns, a reliable wind resource assessment system must include the capability of extracting (i) time series characteristics that reflect the temporal succession of wind speed values, and (ii) time-scale-dependent properties of wind speed patterns. The methodological approach to wind speed pattern analysis presented in this paper not only captures the effects of wind speed value succession, but it considers them on a range of time scales. The paper will first offer details regarding the goals of this approach; subsequently, it will present a method designed to assess scale symmetry properties of time series, after which it will build upon this method and incorporate it into a new, more comprehensive methodology, which determines scale-dependent roughness of wind speed time series. The theoretical aspects are illustrated with concrete analysis examples referring to wind speed records from two different locations.

2. Aim and scope

The aim of this paper is to introduce and illustrate a methodology for wind speed pattern analysis, which is designed to detect, evaluate, and graphically represent time series characteristics that are important to wind power systems, but which are not captured by approaches that are commonly applied in the field of wind energy studies. Wind speed patterns are nonstationary, and their variability extends on a wide range of time scales [17, 18]. Methods specifically developed for the analysis of strongly variable patterns offer fertile avenues towards effective and practically applicable assessment systems [19-22].

To present the proposed approach, we should first note that time series are characterized by two qualitatively different properties: their value distribution, and (assuming that trends and periodicities are removed) their "persistence", which depends on the actual succession of those values [19]. The distribution of wind speed values is usually represented with the help of theoretical distributions such as Weibull, Rayleigh, lognormal, and others; while none of them offers a suitable fit applicable to all situations, the Weibull distribution is often the preferred one [10,23]. The persistence, on the other hand, depends to a large extent on the succession of time series values, which can be considered on different time scales.

Due to wind intermittency, there are times when the turbine rotation slows down, or even ceases altogether. Such events are reflected in the values of wind speed average and the various statistical properties that are used. However, those statistical evaluations are not telling the whole story. After slowdown events or "pauses" in the rotation of a wind turbine, when wind speed increases again, energy is first used to put the rotor in motion and to accelerate the rotation. Energy and time are thus lost not only during time intervals of slow wind, but also during the recovery from weak power output stages. Therefore, counting on the wind power for all the time intervals when the wind speed appears to be high enough, according to the power curve of the turbine, can lead to incorrect results. The number and the temporal distribution of such phenomena are not revealed by the information on average wind speed, or by the statistics that relies on wind speed values alone, without considering their temporal distribution.

For these reasons, it is important to capture time series properties that include both their values and their distribution in time, on a range of scales. The goal of this paper is to produce an effective tool for practical use in relation to wind energy, to complement the existing approaches to wind resource assessment by providing a comprehensive picture of wind patterns – one that captures meaningful aspects of practical importance regarding wind speed variability.

3. Data and Methods

The wind speed data used in this study are provided by AgriMet, Columbia-Pacific Northwest Region, USA, and refer to the time interval 2003-2020, in two stations: Corvallis, Montana (latitude: 46.3 N, longitude: 114.1 W, elevation: 1096 m) and Brookings, Oregon (latitude: 42 N, longitude: 124.2 W, elevation: 24 m). Wind speed data are given at 15 minute-intervals. As an example, a seven-year record for the station of Corvallis is shown in Fig. 1.

The methodology proposed in this paper starts from and incorporates Detrended Fluctuation Analysis, which was proven to get reliable results in a wide variety of applications, especially for nonstationary time series, for which other methods are often affected by errors and biases [22, 24]. This method is briefly described below. The new methodology, which is introduced thereafter, uses the scale-dependent time series variability or "roughness" to generate time vs. temporal scale variability diagrams. The choice of the term "roughness" for these aspects of time series follows the recommendation of the founder of this field of research, Benoit Mandelbrot [25]: a useful review of the areas in which this term is applied in this scholar's ground-breaking work is provided in [26]. Indeed, while scale symmetry properties of time series can be usefully characterized using methods like those described below, the interpretation of results in terms of long-term memory, for instance, is not always helpful. On the contrary, such an interpretation can even be misleading, when it may imply features of the underlying dynamic system, which do not properly describe the studied processes [27]. In this paper the term "roughness" and its quantitative characterization refer to properties of the time series as such, and they are used to compare different segments of data records, time series on different time scales etc.

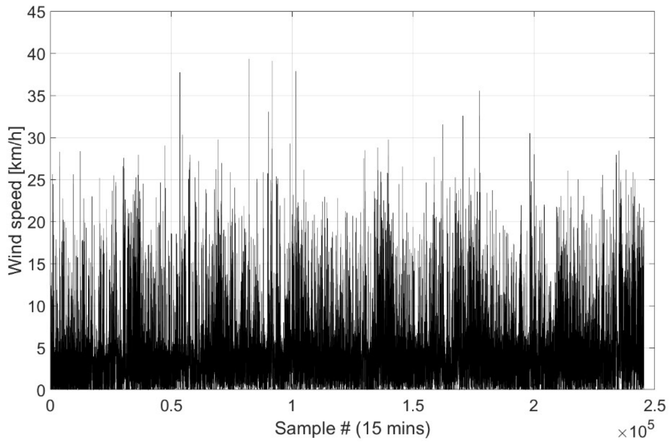

Fig. 1. Wind speed data (15-minute values) recorded in Corvallis, Montana, between July 1st, 2013, and July 1st, 2020.

3.1. Characterizing roughness in time series: method and applications

The first phase of the proposed methodology consists of the analysis of individual time series using Detrended Fluctuation Analysis (DFA), which is a powerful analysis method that has been widely applied to a variety of processes in the environment [28-31].

After normalizing the data, by subtracting the mean and dividing the result by the standard deviation, the time series is divided up in windows of size s, considered in terms of number of samples. The process of dividing the record in windows occurs repeatedly in successive steps, for a series of values of the time scale s. For each time scale s, the "average size of the fluctuation", denoted by F, is determined. Thereby, we obtain a series of pair values, s and $F(s)$. If this relation is a power law:

$$F(s) \propto s^H \tag{1}$$

for a range of time scales s, then the analyzed time series has scale symmetry properties – it is self-affine [19] – over this time scale interval, and its self-affinity is characterized by the exponent H. While the H-exponent is related to the "Hurst exponent", which is determined with other methods [26], it has a distinct meaning, and should thus not be confused with the latter [25]. The H-exponent has values that span the interval (0, 1); time series with H>0.5 are considered persistent, while those with H<0.5 antipersistent. The H-exponent offers a quantitative description of time series roughness, which is associated with a certain range of time scales, as described below. Lower values of H are associated with lower persistence, and thus with a higher roughness of time series.

While this approach is applied in a series of pattern analysis methods, the DFA-specific aspect of this procedure consists of the way in which the "average size of the fluctuation" F is defined. In this case, the best fit polynomial of order N, $P_{N,s}$, is found for each window W_s of length s, and subsequently subtracted from the actual time series in this window. In this study, N=4 was chosen for the polynomial degree, since it led to the narrowest uncertainty intervals; however, values for N = 1 to 7 are all known to provide accurate results [24]. The outcome of this operation is the time series:

$$R_{N,s}(i) = W_s(i) - P_{N,s}(i) \tag{2}$$

The mean of the sum of squares of these differences is then calculated for each window U:

$$F_s^2(U) = \frac{1}{s} \sum_{i=1}^{s} R_{N,s}^2(i) \tag{3}$$

and the square root of the mean of all $F^2(U)$ values gives the average size of the fluctuation for all r windows:

$$F(s) = \left[\frac{1}{r} \sum_{U=1}^{r} F_s^2(U)\right]^{\frac{1}{2}} \tag{4}$$

Two typical examples of the $F(s)$ relation are shown in Fig. 2: the logarithm representation in the diagram emphasizes the linear relationship corresponding to the power law, as per eq. (1). These wind speed records are shown to exhibit a self-affine character, with a roughness given by an H-exponent H=0.34 and of H=0.26, respectively, for these analyzed time series. The obtained H-exponent values had a narrow 95% confidence interval, which is not surprising – the size of this interval is usually lower than 0.01: the linear correlation is strong, with $R^2 > 0.98$. This is the case for most of the analyzed wind speed time series. As shown in Fig. 2, the scale range for the $F(s)$ power law relationship extends from $s = 10^{1.3}$ to $10^{2.5}$ samples (i.e. 20 to 316 samples): since four samples correspond to one hour, the interval of scaling presented in Fig. 2 extends from time scales of five hours to over three days. One can also see from this description that DFA is related to power-spectrum-based methods. However, DFA was proven to be more reliable than spectrum-based methods, especially for nonstationary time series, in which case it is capable of an accurate determination of the *H*-exponent [31]. Since wind speed time series are nonstationary, and an accurate characterization of variability was essential to such studies, it was DFA that was incorporated in the newly designed methodology.

To illustrate the novel, additional nature of the information provided by DFA, compared to the statistical methods mentioned above, we performed the following experiment. We analyzed a time series corresponding to a one-month record of wind speed values, from Corvallis (Fig. 3), according to the method described above. Then, by keeping all wind speed values unchanged, we randomly shuffled the data in the time series, thereby changing the original temporal sequence of these values. The resulted shuffled time series was then subject to the same DFA analysis. Any difference between the results of these two cases, which both contain the same values, must therefore be attributed to the effect of the temporal sequence of values. The results can be seen in Fig. 4. The thin solid line, along with the dotted straight regression line, correspond to the original wind speed time series. The thick solid line and the line-dot regression line belong to the shuffled time series. The difference is striking. The numerical results are even more relevant. The two exponents are: H=0.32 for the original time series, and H=0.03 for the same time series after shuffling the order of the samples.

It should be emphasized that not only do these two time series have the same mean, median, coefficient of variation, etc. They are indiscernible from the point of view of all the mentioned statistical methods applied to wind speed studies, since they consist of the same values. DFA can thus reveal aspects of time series that are indiscernible by the statistical methods that involve time series values, but not their temporal distribution. It is also able to accurately assess patterns without being influenced by nonstationarity. Therefore, it can represent a valuable starting point for the construction of a methodology designed to offer a comprehensive, scale-by-scale view of wind speed variability. The resulting procedure is described below.

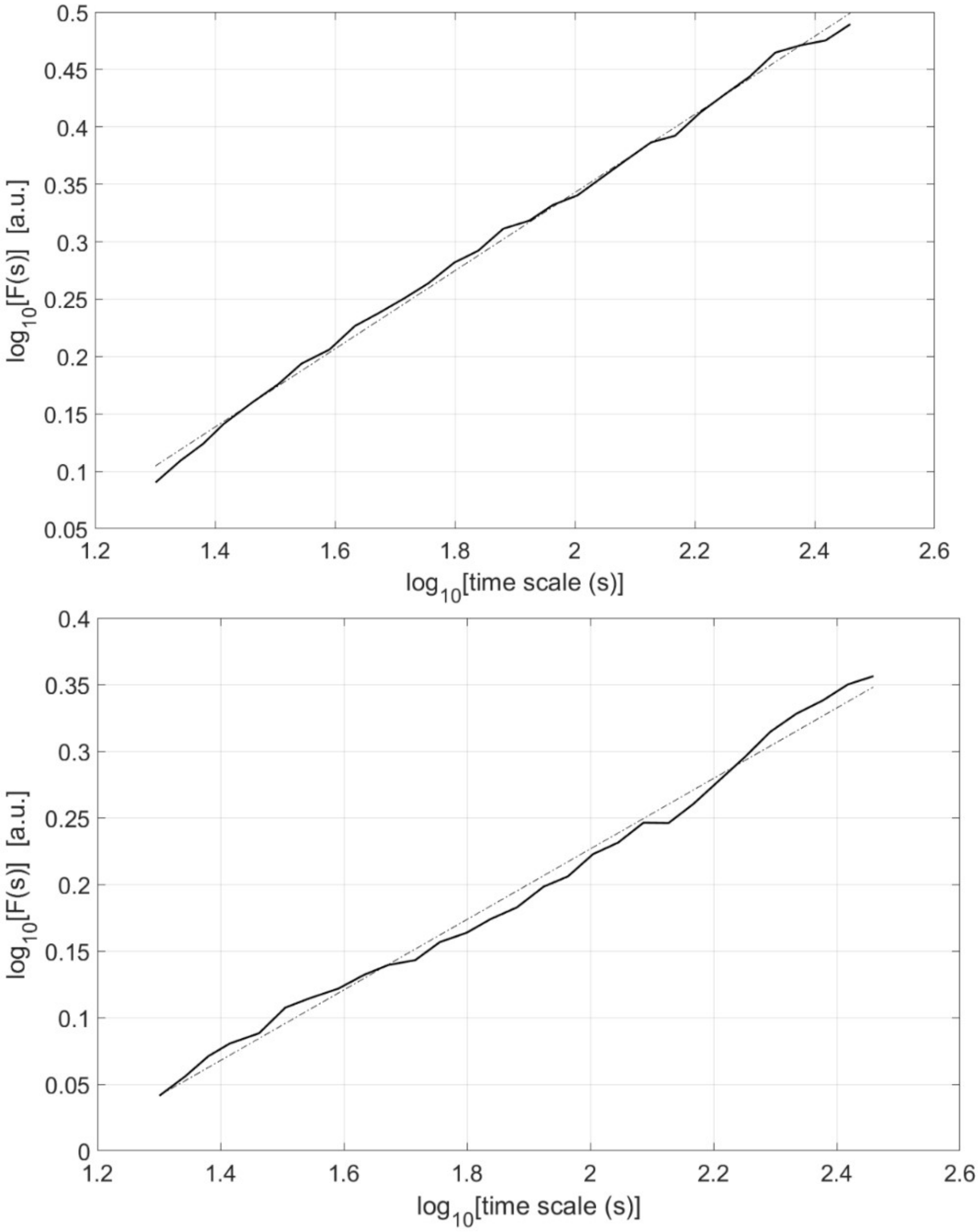

Fig. 2. Two examples of DFA applied to wind speed data recorded in successive months (April and May 2005) in Corvallis, Montana. The dotted line represents the linear regression line.

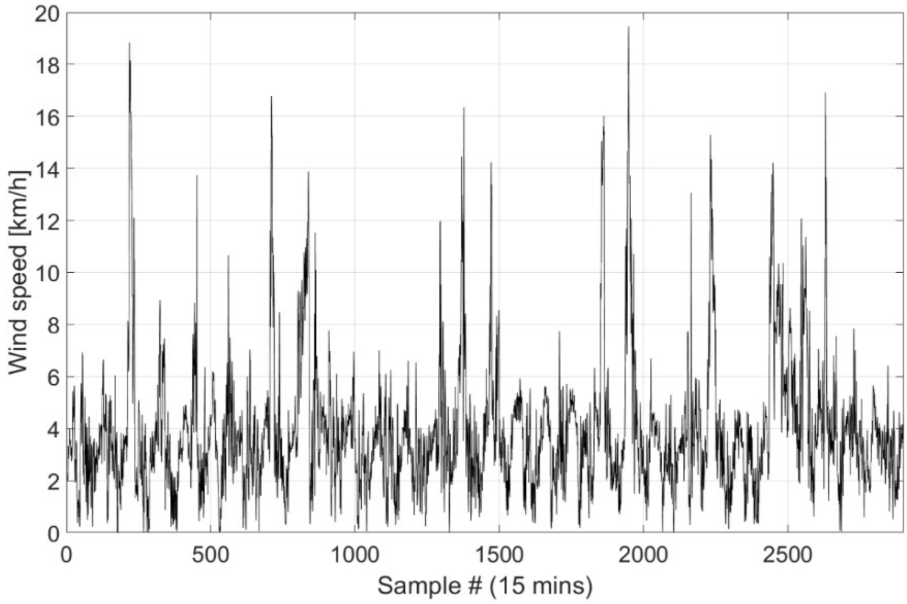

Fig. 3. A one-month segment of the wind speed data record from Corvallis, Montana

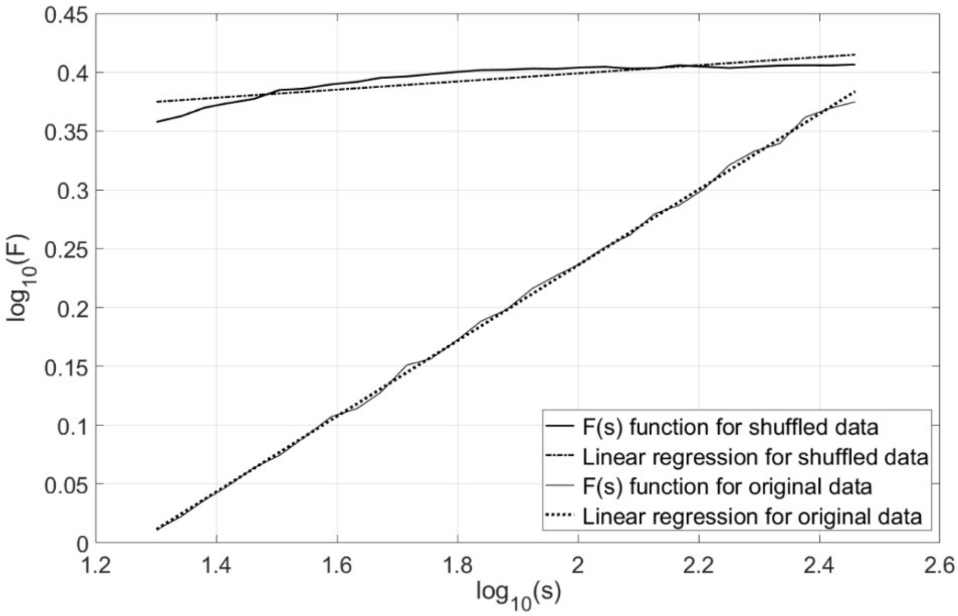

Fig. 4. DFA applied to the original wind speed time series (shown in Fig. 3), and to the same time series after data shuffling. The roughness results prove to critically depend on data succession.

3.2. Time-scale-dependent roughness: isopersistence diagrams

As shown in section 3.1, DFA is capable of reliably producing a quantitative characterization of time series from the point of view of their scale symmetry properties, or self-affinity. It identifies a number, the *H*-exponent, which describes the roughness of the time series on a range of time scales. The goal of this paper is, however, to produce a comprehensive picture of the wind speed variability, so that it can be followed and described both in time and as a function of the time scale.

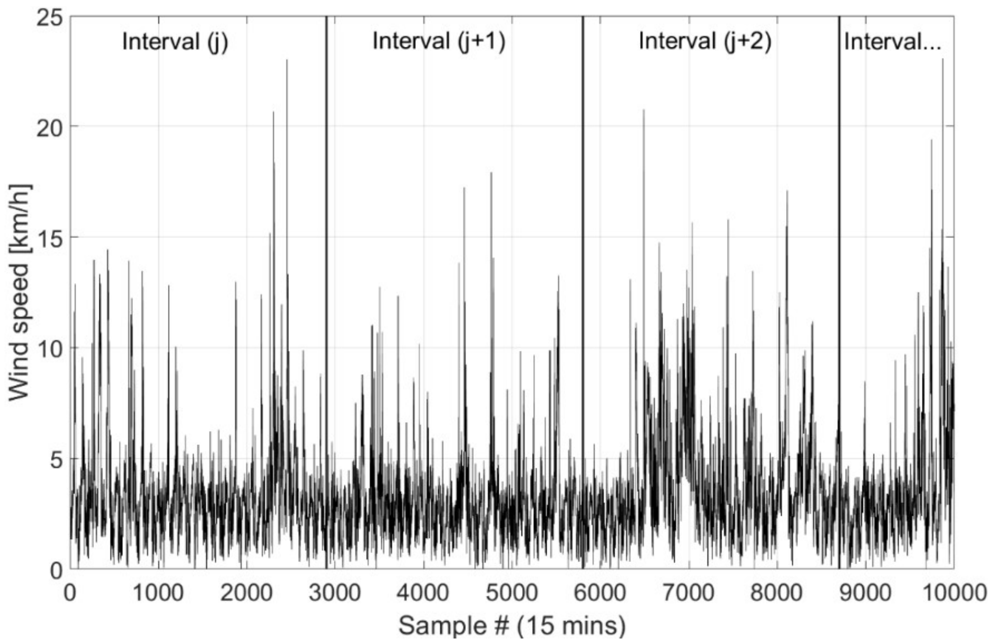

Fig. 5. The first step of the method: splitting the record in a number of intervals (here, of. one month).

To determine the scale-dependent roughness, this new methodology consists of the following steps. After splitting the time series into a number of time intervals, each time interval is subject to DFA analysis. However, instead of stopping after establishing the *H*-exponent, the analysis moves deeper, by looking at the scale-by-scale aspects of the $F(s)$ relation. Following observations from [27], the method calculates the successive slopes for V successive points in the $F(s)$ graph: it applies linear regression to the $\log(s)$ vs. $\log(F)$ relation inside windows of K points that are shifted by one point along the whole graph (Fig. 6).

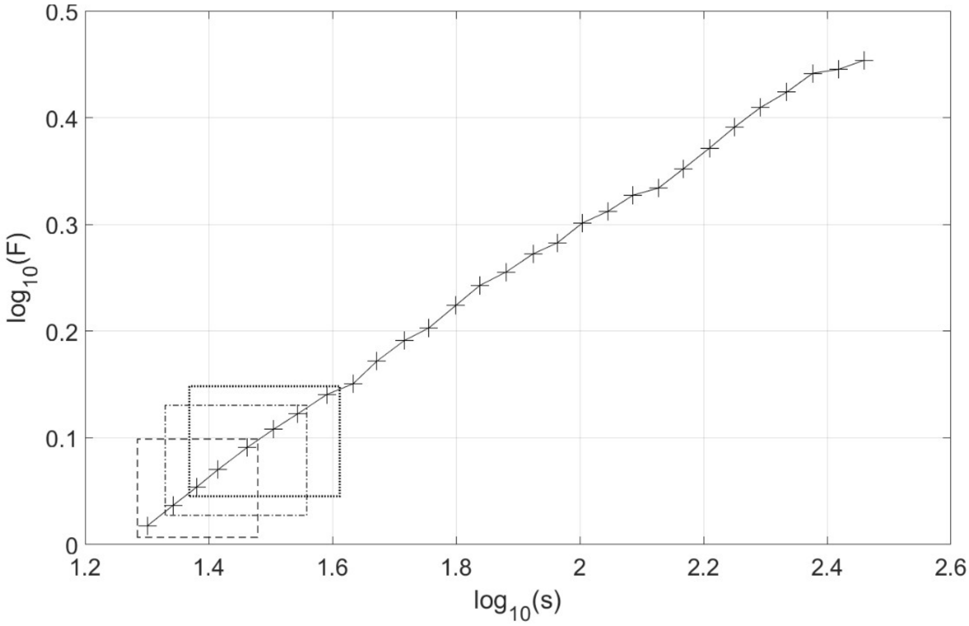

Fig. 6. Determining successive slopes for V-points running interpolation segments (here, V=5). The first three sets of V points are shown.

Instead of only focusing on the successive slope values [32], according to the new method we store these values as a matrix column that corresponds to the analyzed time interval (e.g. one month, one year, etc). This procedure is then applied, in sequence, to all the following time intervals that were produced by splitting up the initial time series (Fig. 5). A set of successive slopes will thus be obtained for each time interval, and inscribed as additional columns to the persistence matrix, W.
The resulting matrix W consists thereafter of the following elements:

$$\begin{array}{lllll} H_{n,q} & H_{n+1,q} & H_{n+2,q} \; \ldots & H_{n+k-1,q} & \text{Longest time scale} \\ H_{n,q-1} & H_{n+1,q-1} & H_{n+2,q-1} \; \ldots & H_{n+k-1,q-1} & \\ H_{n,q-2} & H_{n+1,q-2} & H_{n+2,q-2} \; \ldots & H_{n+k-1,q-2} & \quad\uparrow \\ H_{n,1} & H_{n+1,1} & H_{n+2,1} \; \ldots & H_{n+k-1,1} & \text{Shortest time scale} \\ & & \text{Time} \rightarrow & & \end{array} \tag{5}$$

The indices of H-values have the following meanings:
n is number of the analyzed time interval (e.g. month, year, etc.); the value of n grows from left to right for a total number of k intervals (from n to $n+k-1$);
q is the number of the successive slope values determined for each time segment, based on V-point linear regression in log-log representation (Fig. 6).
In the next stage, the W matrix is shown in a graph: isolines are produced and graphically represented, and the areas they separate are filled according to a colour code. The resulting "persistence landscape" shows values of H-exponents for each time segment and time scale interval. Therefore, contour lines are lines if equal persistence, or isopersistence lines. Using isopersistence diagrams, the time series

variability can be viewed as a function of both time and temporal scale. An illustration of the method is presented below.

4. Results and discussion

The method presented in chapter three is applied to the two specified wind speed datasets: from Corvallis, Montana, and Brookings, Oregon. As shown in chapter 3, the information provided about the time series in terms of self-affinity properties is distinct from the one extracted by the set of statistical methods discussed above. The scale-by-scale approach together with the construction of the persistence matrix based on the analysis of multiple time windows, which represent a novel approach to wind speed patterns, offer a new perspective on wind speed variability (Fig. 7).

The X-axis in this diagram represents time: each vertical slice of the diagram is associated with a time interval. The X-axis density depends on the chosen number (and, in the end, size) of analyzed time intervals (Fig. 6) – months, years, etc., and the length of the available record. The Y-axis represents the q time scales for which H-values were determined based on V-points running segments: in this diagram, they start with $10^{1.38}$ and reach up to $10^{2.38}$ samples, in other words, time scales in these diagrams span an interval between six hours and 2.5 days.

Roughness varies both as a function of time and of temporal scale. These diagrams make it possible to compare, side-by-side, wind patterns in different locations, as well as different time intervals for the same station. On the other hand, they also offer information about the way in which variability changes over time, for any of the studied time scales.

Instead of obtaining merely a number for each time interval, in order to see if and how the determined statistic grows and decreases in time, we benefit from richer information: a two-dimensional surface, on which we can follow or compare variability for any time interval and on any of the studied time scales. As explained in section 3.2., the time scale in isopersistence diagrams (the vertical axis) is the same with the one on the X-axis in the log-log diagrams (Figs. 2, 4, and 6): it is the base 10 logarithm of the size of the time window in number of samples. By analyzing the isopersistence diagram for Corvallis, one can notice an enhanced roughness for certain time scales, such as 2.1 (around 30 days): this feature cannot be found for Brookings. On the other hand, one can identify in both diagrams certain years when the roughness was stronger (2007, 2010, 2016 in both stations), or less strong (2009 and 2019 in both stations, and 2014 in Brookings). Persistence diagrams can also offer clear answers regarding the comparison of variability between two different locations. In the case illustrated here (Fig. 7), wind speed patterns in Brookings prove to have a lower roughness than Corvallis, on the whole range of scales that was studied: the colour bars have the same range in both cases, to facilitate the comparison.

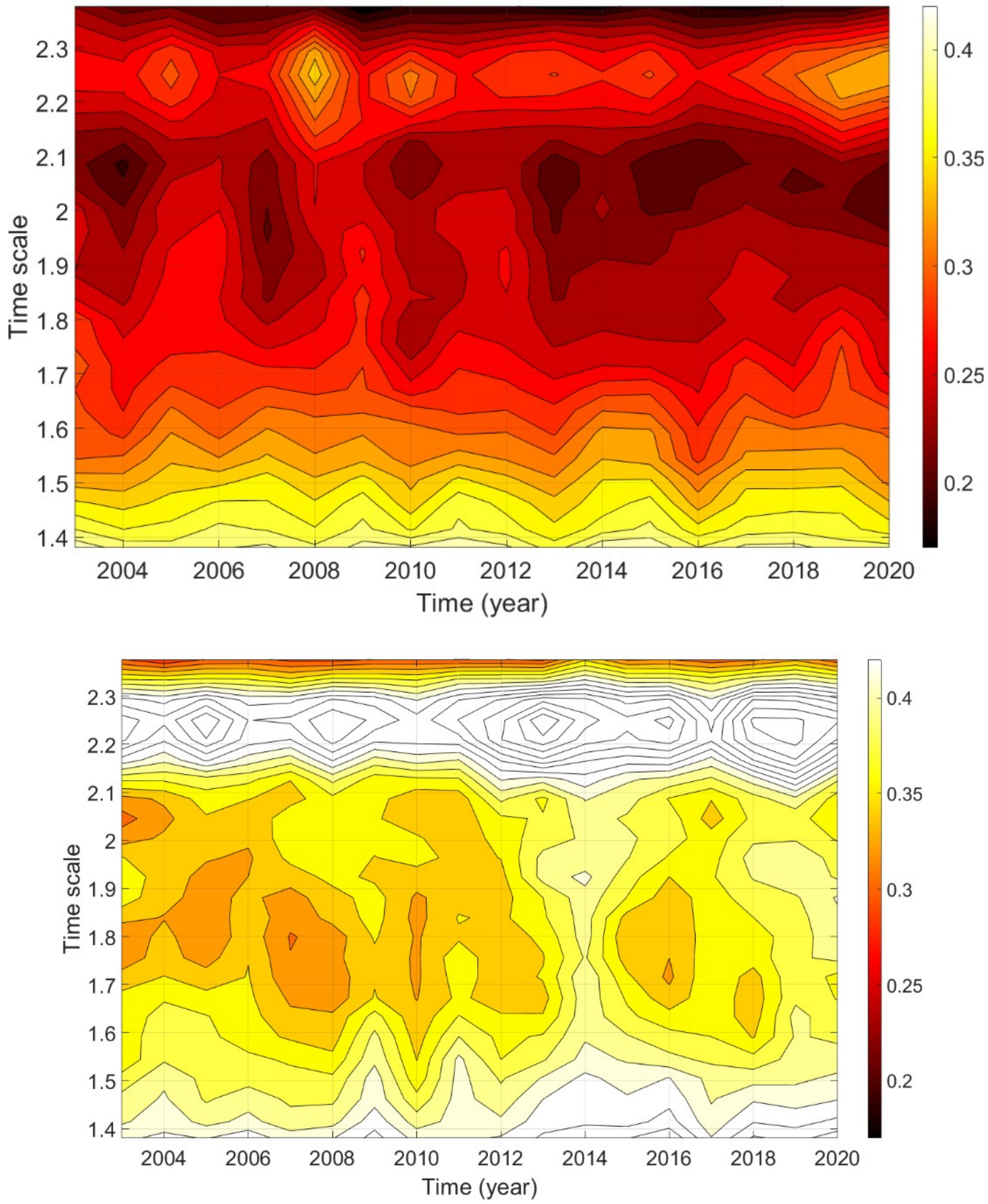

Fig. 7. Isopersistence diagrams for wind speed records from two stations (Corvallis, MT in the upper graph, and Brookings, OR in the lower one). The time scale (base-10 log of sample number) is the same with the X-axis in Figs. 2, 4, and 6. The colour code represents *H*-values: lower values (darker colours) indicate rougher, more variable wind speed patterns.

The proposed methodology makes it also possible to zoom in and zoom out of the diagram, for instance, in order to study certain areas of the roughness landscape in more detail, which offers a flexible approach to the analysis of variability. Although changes in X or Y direction can be made, in principle, independently from each other, certain limits in one direction (such as the minimum length of time windows) can impose constraints regarding changes in the other direction (e.g. temporal scale resolution). However, changes in isopersistence diagram resolution can be independently chosen for the X-axis (time) and the Y-axis (temporal scale) for a wide range of their respective values. To change the X-axis resolution, the analyzed record is divided up in shorter or in longer windows. To change the Y-axis resolution, the number of values for the time scale *s* in the DFA analysis stage is modified accordingly.

5. Conclusions

The wind pattern assessment system presented in this paper offers direct access to accurate information on wind speed variability on a wide range of time scales. It is flexible, easy to use, and adaptable to specific purposes of wind variability analysis, from wind turbine design to insights into the selection of wind turbine locations. The outcome of the system consists of intuitive maps on which one can readily follow and compare information on wind variability as a function of time and temporal scale.

The system introduced and described in this article is not meant to replace proven instruments for wind pattern assessment. It is presented as a potentially useful addition to existing methodological toolboxes, since it is capable of effectively complementing their outcomes with valuable information of practical importance.

Acknowledgements: The author would like to thank AgriMet, Columbia-Pacific Northwest Region, USA, for providing the wind speed data analyzed in this paper.

References

[1] Nikitas G., Bhattacharya S., Vimalan N., Demirci H.E., Nikitas N., Kumar P., *Wind power: A sustainable way to limit climate change*, in Letcher T.M. (ed.), Managing Global Warming. An Interface of Technology and Human Issues, Academic Press, Cambridge, MA, 2019, p. 333-364.

[2] Stern S., Liersch S., Koch H., van Lipzig N.P.M., Thiery W. *A new approach for assessing synergies of solar and wind power: implications for West Africa*, Environmental Research Letters 13:094009, 2018.

[3] World Economic Forum. *The Global Risks Report 2019*, 14th edition, 2019.

[4] Shiau T.-A., Chuen-Yu J.-K., *Developing an indicator system for measuring the social sustainability of offshore wind power farms*, Sustainability, **8**, 2016, p. 470.

[5] Shahriari M., Blumsack S., *Scaling of wind energy variability over space and time*, Applied Energy, **195**, 2017, p. 572-585.

[6] Archer C.L., Jacobson M.Z., *Geographical and seasonal variability of the global "practical" wind resources*, Applied Geography, **45**, 2013, p. 119-130.

[7] Gowrisankaran G., Reynolds S., Samano M., *Intermittency and the Value of Renewable Energy*, Journal of Political Economy, **124**, 4, 2016, p. 1187-1234.

[8] Lund P.D., Byrne J.A., Haas R., Flynn D. (eds.), *Advances in Energy Systems: The Large-scale Renewable Energy Integration Challenge*, Wiley, Hoboken, NJ, 2019.

[9] Lee J.C.Y., Fields M.J., Lundquist J.K., *Assessing variability of wind speed: comparison and validation of 27 methodologies*, Wind Energy Science, **3**, 2018, p. 845-868

[10] Carta J.A., Ramirez P., Velazquez S., *A review of wind speed probability distributions used in wind energy analysis: Case studies in the Canary Islands*, Renewable and Sustainable Energy Reviews, **13**, 5, 2009, p. 933-955.

[11] Kirchner-Bossi N., Garcia-Herrera R., Prieto L., Trigo R.M., *A long-term perspective of wind power output variability*, International Journal of Climatology, **35**, 9, p. 2635-2646.
[12] Kung Ch. – Ch., Chen L. – J., Lee T. – J., Jiang X., Lin R., *Wind power potential for energy sustainability and climate change mitigation: A case study in Taiwan*, Energy & Environment, **30,** 2, 2019, p. 304-321.
[13] Carvalho D., Rocha A., Gomez-Gesteira M., Silva Santos C., *Potential impacts of climate change on European wind energy resource under the CMIP5 future climate projections*, Renewable Energy, **101**, 2017, p. 29-40.
[14] Pryor S. C., Barthelmie R. J., *Climate change impacts on wind energy: A review*, Renew. Sust. Energ. Rev., **14**, 2010, p. 430–437.
[15] Moemken J., Reyers M., Feldmann H., Pinto J.G., *Future changes of wind speed and wind energy potentials in EURO-CORDEX ensemble simulations*, Journal of Geophysical Research: Atmospheres, **123**, 2018, p. 6373-6389.
[16] Rosende C., Sauma E., Harrison G.P., *Effect of climate change on wind speed and its impact on optimal power system expansion planning: The case of Chile*, Energy Economics, **80**, 2019, p. 434-451.
[17] Xu Y.L., Chen J., *Characterizing Nonstationary Wind Speed Using Empirical Mode Decomposition*, Journal of Structural Engineering, **130**, 6, 2004, p. 912.
[18] Solari S., Losada M. A., *Simulation of non-stationary wind speed and direction time series*, Journal of Wind Engineering and Industrial Aerodynamics, **149**, 2016, p. 48-58.
[19] Malamud B.D., Turcotte D.L., *Self-affine time series: I. Generation and analyses*, Advances in Geophysics, **40**, 1999, p. 1-90.
[20] Lovejoy S., Schertzer D., *Haar wavelets, fluctuations and structure functions: convenient choices for geophysics*, Nonlinear Processes in Geophysics, **19**, 2012, p. 513-527.
[21] Lovejoy S., Schertzer D., *The Weather and Climate. Emergent Laws and Multifractal Cascades*, Cambridge University Press, Cambridge, MA, 2013.
[22] Höll M., Kiyono K., Kantz H., *Theoretical foundation of detrending methods for fluctuation analysis such as detrended fluctuation analysis and detrending moving average*, Phys. Rev., **E 99**, 2019, 033305.
[23] Garcia A., Torres J.L., Prieto E., De Francisco A., *Fitting Wind Speed Distributions: A Case Study*, Solar Energy, **62**, 2, 1998, p. 139-144.
[24 Kantelhardt J.W., Koscielny-Bunde E., Rego H.H.A., Havlin S., Bunde A., *Detecting long-range correlations with detrended fluctuation analysis*, Physica A, **295**, 2001, p. 441-454.
[25] Mandelbrot B. B., *Gaussian self-affinity and fractals: Globality, the earth, 1/F noise and R/S*, Selecta, vol. H, Springer-Verlag, New York, 2002.
[26] Watkins N.W., *Mandelbrot's stochastic time series models*, Earth and Space Science, **6 (11)**, 2019, p. 2044-2056.
[27] Maraun D., Rust H.W., Timmer J., *Tempting Long-Memory – on the Interpretation of DFA Results*, Nonlinear Processes in Geophysics, **11**, 2004, p. 495-503.
[28] Tatli H., Dalfes N., *Long-Time Memory in Drought via Detrended Fluctuation Analysis*, Water Resources Management, **34**, 2020, p. 1199–1212.
[29] Jiang L., Zhang J., Fang Y., *Time-Scaling Properties of Sunshine Duration Based on Detrended Fluctuation Analysis over China*, Atmosphere, **10**, 2, 2019, p. 83.
[30] Lennartz S., Bunde A., *Trend evaluation in records with long term memory: application to global warming*, Geophys Res Lett, **36**, 2010, p. L16706
[31] Matsukas Ch., Islam Sh., Rodriguez-Iturbe I., *Detrended fluctuation analysis of rainfall and streamflow time series*, J. Geophysical Research, **105**, D23, 2000, p. 29165-29172.
[32] Suteanu C., *Statistical variability and persistence change in daily air temperature time series from high latitude Arctic stations*, Pure and Applied Geophysics, **172**, 7, 2015, p. 2057-2073.